

AD-A102 905

AIR FORCE GEOPHYSICS LAB HANSCOM AFB MA

F/6 4/1

APPROXIMATE ANALYTIC SOLUTIONS FOR THE PRIMARY AURORAL ELECTRON--ETC(I)

MAR 81 J R JASPERSE, D J STRICKLAND

UNCLASSIFIED AFGL-TR-81-0069

NL

1 OF
AFGL
102 905

END
DATE
9-31
DTIC

AD A102905

LEVEL

12
1.2

AFGL-TR-81-0069
ENVIRONMENTAL RESEARCH PAPERS, NO. 730



Approximate Analytic Solutions for the Primary Auroral Electron Flux and Related Quantities

JOHN R. JASPERSE
D. J. STRICKLAND

DTIC
C AUG 17 1981 D
H

3 March 1981

Approved for public release; distribution unlimited.

SPACE PHYSICS DIVISION
AIR FORCE GEOPHYSICS LABORATORY
HANSCOM AFB, MASSACHUSETTS 01731

AIR FORCE SYSTEMS COMMAND, USAF



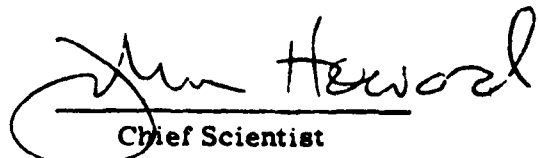
81 8 17 053

X FILE COPY
X

This report has been reviewed by the ESD Information Office (OI) and is releasable to the National Technical Information Service (NTIS).

This technical report has been reviewed and is approved for publication.

FOR THE COMMANDER



Dr. Heward
Chief Scientist

Qualified requestors may obtain additional copies from the Defense Technical Information Center. All others should apply to the National Technical Information Service.

(17) AFGL-TR-81-0069
 AFGL-ERP-730

(12)

Unclassified

SECURITY CLASSIFICATION OF THIS PAGE (When Data Entered)

REPORT DOCUMENTATION PAGE		READ INSTRUCTIONS BEFORE COMPLETING FORM	
1. REPORT NUMBER	2. GOVT ACCESSION NO.	3. PECIORITY	4. LOG NUMBER
AFGL-TR-81-0069	AD-A102905		
5. TITLE (and subtitle)	6. PERFORMING ORG. REPORT NUMBER		
APPROXIMATE ANALYTIC SOLUTIONS FOR THE PRIMARY AURORAL ELECTRON FLUX AND RELATED QUANTITIES	ERP No. 730		
7. AUTHOR(s)	8. CONTRACT OR GRANT NUMBER(s)		
John R. Jaspere* D.J. Strickland*			
9. PERFORMING ORGANIZATION NAME AND ADDRESS	10. PROGRAM ELEMENT, PROJECT, TASK AREA & WORK UNIT NUMBERS		
Air Force Geophysics Laboratory (PHY) Hanscom Air Force Base Massachusetts 01731	611027 2310G601 (17) G6		
11. CONTROLLING OFFICE NAME AND ADDRESS	12. REPORT DATE		
Air Force Geophysics Laboratory (PHY) Hanscom Air Force Base Massachusetts 01731	3 March 1981 (11)		
13. NUMBER OF PAGES	14. SECURITY CLASS. (of this report)		
38	Unclassified		
15. DECLASSIFICATION/DOWNGRADING SCHEDULE			
16. DISTRIBUTION STATEMENT (of this Report)	Approved for public release; distribution unlimited.		
17. DISTRIBUTION STATEMENT (of the abstract entered in Block 20, if different from Report)			
18. SUPPLEMENTARY NOTES			
* Science Applications, Inc., Vienna, VA 22180			
19. KEY WORDS (Continue on reverse side if necessary and identify by block number)			
Linear transport theory Auroral electron flux Auroral energy deposition rate			
20. ABSTRACT (Continue on reverse side if necessary and identify by block number)	In this paper we show that the linear transport equation may be solved exactly for the primary auroral electron flux in plane-parallel geometry in the forward scattering and average, discrete, energy-loss approximations. In this approximation inelastic scattering is taken into account but elastic scattering drops out and the solution is an approximation to the flux in the downward hemisphere. Using the multiple scattering method, we obtain the solution as a finite sum of analytic functions of altitude, energy, and pitch angle where		

DD FORM 1 JAN 73 EDITION OF 1 NOV 85 IS OBSOLETE

Unclassified

SECURITY CLASSIFICATION OF THIS PAGE (When Data Entered)

404518 901

Unclassified

Do Not Use This Page When Data Entered

20. Abstract (Continued)

each term is multiplied by the energy shifted electron flux incident at the top of the auroral ionosphere. Closed form expressions are also found for the hemispherically averaged primary electron flux, the energy deposition rate, and the ionization rate. For a unidirectional incident flux we show that the energy deposition rate is a superposition of generalized Chapman functions of altitude, and for an isotropic incident flux we show that the energy deposition rate is a superposition of generalized J functions of altitude. The notion of pseudoparticles is discussed and used to approximate the sums which occur in the above formulae. We also compare our analytic approximations to some numerical solutions of the problem.

Unclassified

Do Not Use This Page When Data Entered

Preface

The authors wish to thank Dr. A. L. Snyder for support and encouragement throughout the course of the work and Mr. N. Grossbard who performed some of the calculations for this paper.

Classification For	
NTIS GRA&I	<input checked="" type="checkbox"/>
DODIC T&B	<input type="checkbox"/>
Uncontrolled	<input type="checkbox"/>
Justification	
By _____	
Distribution/	
Availability Codes	
Date Entered _____	
Distr. Control No. _____	
	

Contents

1. INTRODUCTION	7
2. BASIC EQUATION	10
3. EQUATION FOR THE PRIMARY ELECTRON FLUX	10
4. FORWARD SCATTERING AND AVERAGE DISCRETE ENERGY-LOSS APPROXIMATIONS	11
5. MULTIPLE SCATTERING METHOD	14
6. MULTIPLE SCATTERING SOLUTION	15
7. HEMISPHERICALLY AVERAGED FLUX, ENERGY DEPOSITION RATE AND IONIZATION RATE	18
8. SOLUTIONS FOR SPECIFIC INCIDENT ELECTRON FLUXES	18
8.1 Preliminary Remarks	18
8.2 Unidirectional-Monoenergetic Incident Flux	19
8.3 Isotropic-Maxwellian Incident Flux	20
8.4 Isotropic-Monoenergetic Incident Flux	21
9. RELATIONSHIP BETWEEN THE ENERGY DEPOSITION RATE AND CHAPMAN AND J FUNCTIONS	22
9.1 Preliminary Remarks	22
9.2 Generalized Chapman and J Functions	23
9.3 Energy Deposition Rate for Unidirectional Incident Fluxes	24
9.4 Energy Deposition Rate for Isotropic Incident Fluxes	25
10. USE OF PSEUDOPARTICLES TO APPROXIMATE THE SUMS	25

Contents

11. COMPARISONS	28
11.1 Preliminary Remarks	28
11.2 Comparisons for Isotropic-Monoenergetic Incident Fluxes	29
11.3 Comparisons for Isotropic-Maxwellian Incident Fluxes	31
12. CONCLUSIONS	33
REFERENCES	37

Illustrations

1. Hemispherically Averaged Partial Fluxes for an Isotropic Maxwellian with $E_0 = 2 \text{ KeV}$, $Q_s = 1 \text{ erg/cm}^2 \text{ s}$ and $N = 12$	6
2. Sequence of Partial Sums of Hemispherically Averaged Partial Fluxes for an Isotropic-Maxwellian as in Figure 1	27
3. Partial Ionization Rates for an Isotropic-Maxwellian with $E_0 = 2 \text{ KeV}$, $Q_s = 1 \text{ erg/cm}^2 \text{ s}$ and $N = 12$	27
4. Sequence of Partial Sums of Partial Ionization Rates for an Isotropic-Maxwellian as in Figure 3	28
5. Energy Deposition Rates from the Analytic, Range, and Rees Models for 10, 5, and 2 KeV Isotropic-Monoenergetic Sources Each Containing $1 \text{ erg/cm}^2 \text{ s}$	30
6. Incident Maxwellian Energy Distributions for Characteristic Energies of 5, 2, and 1 KeV Each Containing $1 \text{ erg/cm}^2 \text{ s}$	31
7. Energy Deposition Rates from the Analytic, Range, and Strickland Models for the 5, 2, and 1 KeV Isotropic-Maxwellian Sources as in Figure 6	32
8. Differential Electron Fluxes from the Analytic ($N = 12$) and Strickland Models at 110 km for the 2 KeV Isotropic-Maxwellian Source	34
9. Hemispherically Averaged Fluxes from the Analytic ($N = 12$) and Strickland Models at 110 and 160 km for the 2 KeV Isotropic-Maxwellian Source	35

Approximate Analytic Solutions for the Primary Auroral Electron Flux and Related Quantities

I. INTRODUCTION

The problem of calculating the distribution function for auroral electrons may be approached from two points of view. One approach is to neglect collective effects and treat short range particle-particle collisions using linear transport theory; the other is to neglect short range collisions and treat collective effects using quasilinear or nonlinear plasma kinetic theory. At high altitudes the latter approach is often used as the plasma is essentially collisionless, whereas at low altitudes (below about 250 km) linear transport theory is generally used as the plasma is neutral particle collision dominated. The question of how to combine the short range and collective aspects of the problem is, and should be, an active area of research. In this paper we confine our attention to the lower ionosphere and apply the methods of linear transport theory to calculate the auroral primary electron flux.

There is an extensive literature on the subject of electron transport in the auroral ionosphere. The various approaches may be categorized as semi-empirical, range theoretic, Fokker-Planck, Monte Carlo, and transport theoretic.

Early work on transport properties of KeV auroral electrons comes from Chamberlain.¹ Estimates were made of ionization rates as a function of altitude

(Received for publication 2 March 1981)

1. Chamberlain, J.W. (1961) Physics of Aurora and Airglow, Academic Press, N.Y.

for energetic KeV electrons. The rates were based on deposition results of Spencer who solved the electron transport equation using the continuous energy loss approximation.^{2,3} Rees⁴ (a semi-empirical approach) applied an energy dissipation function based on laboratory data by Grun.⁵ The forms of the functions obtained by Rees provided altitude profiles of the energy deposition and ionization rates for monoenergetic and energy distributed sources with various pitch angle dependences.

Walt et al, were the first to provide altitude, energy, and pitch angle information on auroral electron fluxes in the KeV range.⁶ To do so they obtained a numerical solution of a Fokker-Planck equation which was originally used to study the properties of electrons trapped in the radiation belts.⁷ The method assumes continuous energy loss and small angle scattering. Banks et al,⁸ joined together Walt's Fokker-Planck method and a low energy approximate two-stream transport method by Banks and Nagy,⁹ previously applied to photoelectron transport. The resulting equation was solved numerically.

Beger et al, chose to examine auroral electron transport by applying Monte Carlo techniques.^{10,11} Backscatter yields, backscatter spectra, and altitude profiles of the energy deposition rate are among the transport quantities that were calculated by this method. In the first of the two papers noted above, information was also given on the lateral spreading of KeV, narrow electron beams.

2. Spencer, L. V. (1955) Theory of electron penetration, Phys. Rev. 98:1597.
3. Spencer, L. V. (1959) Energy dissipation by fast electrons, National Bureau of Standards Monograph 1.
4. Rees, M. H. (1963) Auroral ionization and excitation of incident energetic electrons, Planet. Space Sci. 11:1209.
5. Grun, A. E. (1957) Lumineszenz-photometrische messungen der energieabsorption im strahlungsfeld von electronquellen, eindimensionaler fall in luft, Z. Naturforsch., Ser. A, 12:89.
6. Walt, M., MacDonald, W. M., and Francis, W. E. (1967) Penetration of auroral electrons into the atmosphere, Physics of the Magnetosphere, R. L. Carovillano, J. F. McClay, and H. R. Radoski, eds., D. Reidel, Dordrecht, Netherlands, 534.
7. MacDonald, W. M. and Walt, M. (1961) Distribution function of magnetically confined electrons in a scattering atmosphere, Ann. Phys. 15:44.
8. Banks, P. M., Chappell, C. R., and Nagy, A. F. (1974) A new model for the interaction of auroral electrons with the atmosphere: Spectral degradation backscatter, optical emission, and ionization, J. Geophys. Res. 79:1459.
9. Banks, P. M. and Nagy, A. F. (1970) Concerning the influence of elastic scattering upon photoelectron transport and escape, J. Geophys. Res. 75:1902.
10. Berger, M. J., Seltzer, S. M., and Maeda, K. (1970) Energy deposition by auroral electrons in the atmosphere, J. Atmos. Terr. Phys. 32:1015.
11. Berger, M. J., Seltzer, S. M., and Maeda, K. (1974) Some new results on electron transport in the atmosphere, J. Atmos. Terr. Phys. 36:591.

There are at least three transport models utilizing the linear transport equation which have recently been applied to auroral studies. These are the models of Strickland et al,¹² Mantas¹³ and Stammes.¹⁴ All three models give a detailed description of elastic scattering and allow for discrete energy loss. Differences arise in the representation of the flux within the collision integral and in the method of integration over depth. Strickland et al, allow the flux to vary quadratically in $\ln E$ and linearly in μ within any given E, μ cell.¹² The quadratic dependence was introduced because of energy conservation problems for a linear dependence when treating energetic fluxes above several KeV. The integration over depth is carried out by either a finite difference method (second order predictor-corrector) or an eigenvalue method. The latter approach was found to be much faster and more accurate. Mantas allows the flux to vary linearly in both E and μ within any E, μ cell.¹³ He also uses a linear dependence within a given z cell which leads to the standard finite difference expression for the first order z derivatives. Stammes treats the μ dependence of the problem by the discrete ordinate method and considers the flux to be constant within a given E cell (commonly called the multigroup approximation).¹⁴ For a good discussion of the discrete ordinate and multigroup methods see Davison.¹⁵ Like Strickland et al,¹² Stammes uses an eigenvalue technique to carry out the integration over depth. The discrete ordinate method for treating the angular dependence of the electron flux converges poorly for highly anisotropic scattering kernels. Therefore, the angular dependence of the results of Stammes at high energies in the backward direction are questionable. All of the transport methods lead to a truncated matrix equation which is solved numerically.

The new feature of the work presented by us in this paper is that we give approximate analytic solutions for the primary auroral electron flux in the downward hemisphere and related quantities. All previous work on this problem has resulted in numerical solutions. The analytic results, though approximate, are useful in giving insight into the physics of auroral electron precipitation and in carrying out further analytical studies of auroral phenomena. For example, in work currently in progress using the multiple scattering method, we show that elastic scattering can be included rigorously and that the solution given in this

- 12. Strickland, D.J., Book, D.L., Coffey, T.P., and Fedder, J.A. (1976) Transport equation techniques for the deposition of auroral electrons, *J. Geophys. Res.* 81:2755.
- 13. Mantas, G.P. (1975) Theory of photoelectron thermalization and transport in the ionosphere, *Planet. Space Sci.* 23:337.
- 14. Stammes, K. (1978) A theoretical investigation of the interaction of auroral electrons with the atmosphere, Ph.D. thesis, University of Colorado, Colorado.
- 15. Davison, B. (1957) Neutron Transport Theory, Oxford Press, London.

paper is just the leading term in an iterative sequence of solutions which treats the complete problem including secondary electron production. In work also in progress the method presented in this paper is used to solve the coupled proton-hydrogen precipitation problem for the proton aurora. These solutions for the proton and hydrogen flux and related quantities are similar to the ones presented here for the electron precipitation problem.

2. BASIC EQUATION

For a one constituent atmosphere the linear transport equation for energetic electrons in plane-parallel geometry is

$$\left[u \frac{\partial}{\partial z} + n(z) Q_t(E) \right] \Phi(z, E, \mu) = n(z) Q_t(E) \int dE' d\mu' R(E'\mu' \rightarrow E\mu) \Phi(z, E', \mu') , \quad (1)$$

where Φ is the electron flux, n is the neutral density, and

$$R(E'\mu' \rightarrow E\mu) \equiv \frac{2\pi}{Q_t(E)} \sum_j \sigma_j(E'\mu' \rightarrow E\mu) . \quad (2)$$

Here, z is the altitude, E the particle energy, μ the cosine of the angle between the particle velocity and the positive z -axis, and σ_j the differential cross section per unit energy range (referred to hereafter as the differential cross section) for electron-neutral particle scattering where the neutral particle makes a transition from the ground state to the final state j . The total cross section, $Q_t(E)$, is related to the differential cross section by the formula

$$Q_t(E) = 2\pi \int dE' d\mu' \sum_j \sigma_j(E\mu \rightarrow E'\mu') . \quad (3)$$

3. EQUATION FOR THE PRIMARY ELECTRON FLUX

The differential cross sections describe elastic, excitation, and ionization-type collisions between the electrons and the neutral particles. In ionization-type collisions additional (secondary) electrons are produced. The electron flux in Eq. (1) includes both primary and secondary electrons. The secondary electron

spectrum is highly peaked at low energies ($< E_{\min}$) with very few secondary electrons at higher energies ($> E_{\min}$).¹⁶ In the auroral ionosphere E_{\min} is somewhat arbitrary but is on the order of 1/2 KeV for primary electrons ranging from 1 to 60 KeV. If we restrict the energy range of Eq. (1) to high energies, we may approximate the electron flux by neglecting the secondaries compared to the primaries; that is,

$$\Phi \sim \Phi_{\text{primaries}} \quad \text{for} \quad E > E_{\min} \quad , \quad (4)$$

and use a differential cross section for ionization-type collisions that describes only the scattering of the primary electrons. Viewing the ionization-type collisions in this way we may approximate the differential cross sections for KeV auroral electrons by

$$\sigma_e(E^t \mu^+ \rightarrow E_\mu) \sim (2\pi)^{-1} Q_e(E^t) \delta(E^t - E) p_e(E^t, \mu^+, \mu^-) \quad , \quad (5)$$

$$\sigma_{\text{exk}}(E^t \mu^+ \rightarrow E_\mu) \sim (2\pi)^{-1} Q_{\text{exk}}(E^t) \delta[E^t - (E + W_k)] p_{\text{exk}}(\mu^+, \mu^-) \quad , \quad (6)$$

$$\sigma_{if}^{(p)}(E^t \mu^+ \rightarrow E_\mu) \sim (2\pi)^{-1} \sigma_{if}^{(p)}(E^t, E) p_{if}^{(p)}(\mu^+, \mu^-) \quad . \quad (7)$$

Here, the subscripts e, ex, and if refer to elastic, excitation, and ionization-type collisions, respectively, δ is the Dirac delta function, the p functions are symmetric in μ^+ and μ^- and are normalized to one, the total cross section for each process is denoted by Q , and the superscript p refers to primary electrons. W_k is the excitation energy. For a discussion of the elastic, excitation, and ionization type cross sections see Strickland et al.¹⁷

The equation for the primary electron flux is Eq. (1) with the differential cross sections given by Eqs. (5), (6), and (7), and is valid for $E > E_{\min}$.

4. FORWARD SCATTERING AND AVERAGE DISCRETE ENERGY-LOSS APPROXIMATIONS

In the auroral region two facts about the differential cross sections at high energies are apparent. They are that 1) the differential cross sections are highly peaked in the forward direction, the excitation, and ionization type collisions being

16. Opal, C.B., Peterson, W.K., and Beatty, E.C. (1971) Measurements of secondary-electron spectra produced by electron impact ionization of a number of simple gases, J. Chem. Phys., 55:4100.

even more highly peaked than the elastic collisions, and 2) the average energy loss per inelastic collision (excitation and ionization) is a weak function of the incident electron energy. This suggests that for inelastic collisions we make the forward-scattering and average discrete energy-loss approximations:

$$\sum_k \sigma_{exk}(E'\mu' \rightarrow E\mu) \rightarrow (2\pi)^{-1} \left(\sum_k Q_{exk}(E') \right) \delta[E' - (E + W)] \delta(\mu' - \mu) , \quad (8)$$

$$\sum_\ell \sigma_{il}^{(p)}(E'\mu' \rightarrow E\mu) \rightarrow (2\pi)^{-1} \left(\sum_\ell Q_{il}(E') \right) \delta[E' - (E + W)] \delta(\mu' - \mu) , \quad (9)$$

where W is the average primary electron energy lost per inelastic collision defined by

$$W \equiv \left[\sum_k W_k Q_{exk}(E) + \sum_\ell \int dE'(E - E') \sigma_{il}^{(p)}(E, E') \right]^{-1} \times \left[\sum_k Q_{exk}(E) + \sum_\ell \int dE' \sigma_{il}^{(p)}(E, E') \right] . \quad (10)$$

W as a function of E for the auroral cross sections used by Strickland et al. is 32, 36, 42 and 48 in eV for 1, 3, 10 and 30 KeV primary electron energies, respectively.¹² In the average discrete energy-loss approximation W is assumed constant. For elastic cross sections a screened Rutherford cross section is often used:

$$\sigma_e(E'\mu' \rightarrow E\mu) \rightarrow (2\pi)^{-1} Q_e(E') \delta(E' - E) p(\eta, \mu', \mu) , \quad (11)$$

$$p(\eta, \mu', \mu) = \frac{2\eta(1+\eta)(1+2\eta-\mu'\mu)}{[(1+2\eta-\mu'\mu)^2 - (1-\mu'^2)(1-\mu^2)]^{3/2}} , \quad (12)$$

where η is a function of energy. For graphs of p as a function of η , μ' and μ , and η as a function of E see Strickland et al.¹²

Inserting Eq. (8) through Eq. (12) into Eq. (1) and transforming Eq. (1) to an equation in terms of the optical depth, τ , where

$$d\tau = -n(z) Q(E) dz \quad , \quad (13)$$

we obtain

$$\begin{aligned} \left(-\mu \frac{\partial}{\partial \tau} + 1 \right) \Phi(\tau, E, \mu) &= \frac{Q(E + W)}{Q(E)} \Phi(\tau(z, E + W), E + W, \mu) \\ &+ \frac{Q_e(E)}{Q(E)} \left[-\Phi(\tau, E, \mu) + \int_{-1}^{+1} d\mu' p(\eta, \mu', \mu) \Phi(\tau, E, \mu') \right] \quad , \end{aligned} \quad (14)$$

where Q and Q_e denote the total inelastic and total elastic cross sections, respectively, and τ denotes $\tau(z, E)$. The ratio $Q(E + W)/Q(E)$ is near 1 and the ratio $Q_e(E)/Q(E)$, as given by Strickland et al., is 0.84, 0.62, 0.45 and 0.37 for 1, 3, 10 and 30 KeV primary electron energies, respectively.¹² On the right-hand side of Eq. (14) we may view the second and third terms as producing a correction to the first term. This correction is not necessarily small. For example, we know that in the backward hemisphere elastic scattering is the dominate process and contributes the most to the backscattered flux. The solution here is very sensitive to the ratio Q_e/Q and to the precise shape of $p(\eta, \mu', \mu)$. However, in the downward hemisphere we expect the first term on the right-hand side of Eq. (14) to produce a contribution to Φ which is comparable to or larger than the contribution made by the second and third terms. In this paper we seek an approximation to the flux in the downward hemisphere. An equation for such an approximate solution is obtained from Eq. (14) by taking the limit of the function p as $E \rightarrow \infty$ ($\eta \rightarrow 0$). It can be shown that

$$p(\eta, \mu', \mu) \xrightarrow[\eta \rightarrow 0]{} \delta(\mu' - \mu) \quad . \quad (15)$$

In the high-energy approximation elastic scattering becomes highly peaked in the forward direction and drops out of Eq. (14). We obtain

$$\left(-\mu \frac{\partial}{\partial \tau} + 1 \right) \Phi(\tau(z, E), E, \mu) = \frac{Q(E + W)}{Q(E)} \Phi(\tau(z, E + W), E + W, \mu) \quad . \quad (16)$$

Equation (16) is a partial differential-difference equation for the primary electron flux now denoted by Φ , as a function of τ , E and μ , approximately valid for $0 \leq \tau < \infty$, $E_{\min} \leq E < \infty$, and $-1 \leq \mu < 0$.

5. MULTIPLE SCATTERING METHOD

The multiple scattering method may be applied in principle to any linear transport equation satisfying certain general requirements. For a discussion of the multiple scattering method applied to elastic scattering see Goudsmit and Saunderson,¹⁷ and Wang and Guth,¹⁸ to inelastic scattering see Fano,¹⁹ and to both types of scattering see Case and Zweifel.²⁰ In our case we wish to apply it to Eq. (16) which contains only inelastic scattering. To do so we rewrite Eq. (16) as

$$\left(-\mu \frac{\partial}{\partial \tau} + 1 \right) \Phi = \mathcal{L}\Phi , \quad (17)$$

where \mathcal{L} is the linear operator that shifts the energy variable of Φ by W and multiplies by $Q(E + W)/Q(E)$. The multiple scattering method consists of writing

$$\Phi(\tau, E, \mu) = \sum_{n=0}^{\infty} \phi_n(\tau, E, \mu) , \quad (18)$$

where the ϕ_n satisfy the infinite system of equations

$$\left(-\mu \frac{\partial}{\partial \tau} + 1 \right) \phi_0 = 0 , \quad (19)$$

$$\left(-\mu \frac{\partial}{\partial \tau} + 1 \right) \phi_1 = \mathcal{L}\phi_0 , \quad (20)$$

- 17. Goudsmit, S. and Saunderson, J. L. (1940) Multiple scattering of electrons, Phys. Rev. 57:24.
- 18. Wang, M. C. and Guth, E. (1951) On the theory of multiple scattering, particularly of charged particles, Phys. Rev. 84:1092.
- 19. Fano, U. (1953) Degradation and range straggling of high-energy radiations, Phys. Rev. 92:330.
- 20. Case, K. M. and Zweifel, P. L. (1967) Linear Transport Theory, Addison-Wesley, Reading, 48.

$$\left(-\mu \frac{\partial}{\partial \tau} + 1 \right) \phi_n = \phi_{n-1} , \quad (21)$$

and then solving for the ϕ_n subject to appropriate boundary conditions. If Φ exists it is referred to as the multiple scattering or orders of scattering solution. The fact that Eq. (18) is a solution to Eq. (17) is seen by adding the above infinite system of equations for the ϕ_n .

The function ϕ_n which we may call the nth order partial flux has a simple physical interpretation. ϕ_0 is the flux of particles per unit energy per unit solid angle at z , E , and μ which have experienced no collisions, ϕ_1 is the flux of particles per unit energy per unit solid angle at z , E , and μ which have scattered once, and so on for each order of scattering denoted by n .

6. MULTIPLE SCATTERING SOLUTION

The boundary condition for electrons incident at the top of the ionosphere is

$$\Phi(0, E, \mu) = \Phi(E, \mu) , \quad \text{for } -1 \leq \mu < 0 . \quad (22)$$

This implies that for $n = 0$,

$$\phi_0(0, E, \mu) = \Phi(E, \mu) , \quad \text{for } -1 \leq \mu < 0 , \quad (23)$$

and for $n \geq 1$,

$$\phi_n(0, E, \mu) = 0 , \quad \text{for } -1 \leq \mu < 0 . \quad (24)$$

No particles are incident from below the ionosphere.

The solution to Eq. (16) may be found as follows. The solution for ϕ_0 subject to the above boundary condition is

$$\phi_0(\tau, E, \mu) = \begin{cases} \Phi(E, \mu) \exp(\tau/\mu) , & -1 \leq \mu < 0 \\ 0 , & 0 \leq \mu \leq 1 \end{cases} \quad (25)$$

and the solution ϕ_n in terms of ϕ_{n-1} for $n \geq 1$ is

$$\phi_n(\tau, E, \mu) = -\exp(\tau/\mu) \int_0^\tau dt \mu^{-1} b_{11} \phi_{n-1}(b_{11}t, E + W, \mu) \exp(-t/\mu) , \quad (26)$$

for $-1 \leq \mu < 0$. For $0 \leq \mu \leq 1$ the ϕ_n are zero. The complete solution is

$$\begin{aligned} \Phi(\tau, E, \mu) &= \Phi(E, \mu) \exp(\tau/\mu) + \sum_{n=1}^{\infty} \Phi(E + nW, \mu) b_{n1}(E) \\ &\times [H_n(\tau/\mu, E) - H_n(0, E) \exp(\tau/\mu)] , \end{aligned} \quad (27)$$

for $-1 < \mu < 0$, and $\Phi = 0$ for $0 \leq \mu \leq 1$. The recursion relation for the H functions is

$$\begin{aligned} \exp(-x) H_{n+1}(x, E) - H_{n+1}(0, E) &= \\ - \int_0^x dx' \exp(-x') [H_n(b_{11}x', E + W) - H_n(0, E + W) \exp(b_{11}x')] & . \end{aligned} \quad (28)$$

An explicit formula for the general H function has been worked out by mathematical induction but, as it is quite lengthy, only the first three functions will be given here:

$$H_1(x, E) = a_{11} \exp(b_{11}x) , \quad (29)$$

$$H_2(x, E) = a_{22}a_{21} \exp(b_{21}x) - a_{22}a_{11} \exp(b_{11}x) , \quad (30)$$

$$\begin{aligned} H_3(x, E) &= a_{33}a_{32}a_{31} \exp(b_{31}x) - a_{33}a_{32}a_{11} \exp(b_{11}x) \\ &- a_{33}a_{22}a_{21} \exp(b_{21}x) + a_{33}a_{22}a_{11} \exp(b_{11}x) . \end{aligned} \quad (31)$$

In the above formulae we have introduced the following definitions:

$$b_{nm} - b_{nm}(E) = Q(E + nW)/Q(E + (m - 1)W) , \quad (32)$$

$$a_{nm} = a_{nm}(E) \equiv [1 - b_{nm}(E)]^{-1} . \quad (33)$$

Equation (27) may be rewritten in an alternative form as

$$\Phi(\tau, E, \mu) = \Phi(E, \mu) \exp(\tau/\mu) + \sum_{n=1}^{\infty} \Phi(E + nW, \mu) \sum_{\ell=1}^n A_{n\ell} \times [\exp(B_\ell \tau/\mu) - \exp(\tau/\mu)] , \quad (34)$$

where

$$B_\ell(E) = B_\ell \equiv b_{\ell 1}(E) , \quad (35)$$

and the first few $A_{n\ell} \equiv A_{n\ell}(E)$ are

$$A_{11} = + b_{11} a_{11} , \quad (36)$$

$$A_{22} = + b_{21} a_{22} a_{21} , \quad (37)$$

$$A_{21} = - b_{21} a_{22} a_{11} , \quad (38)$$

$$A_{33} = + b_{31} a_{33} a_{32} a_{31} , \quad (39)$$

$$A_{32} = - b_{31} a_{33} a_{22} a_{21} , \quad (40)$$

$$A_{31} = - b_{31} [+ a_{33} a_{32} a_{11} - a_{33} a_{22} a_{11}] . \quad (41)$$

Several comments about this solution are in order. The primary electron flux, Φ , is an exact solution to Eq. (16) which is in turn an approximation to Eq. (1). The fact that it solves Eq. (16) exactly can be verified by direct substitution. The value of Φ depends linearly on its boundary value; doubling the incident flux doubles the flux at all altitudes. The solution yields no backscattered primary electron flux. The reason for this is that in the forward scattering approximation elastic scattering drops out and no particles are scattered into the backward direction.

7. HEMISPHERICALLY AVERAGED FLUX, ENERGY DEPOSITION RATE AND IONIZATION RATE

The hemispherical electron flux, Φ_H , is defined as the average value of the electron flux over the downward hemisphere and is

$$\Phi_H(\tau, E) \equiv 2\pi \int_{-1}^0 d\mu \Phi(\tau, E, \mu)/2\pi . \quad (42)$$

The energy deposition rate, η_E , is defined as the energy deposited per unit volume per unit time by the precipitating electrons, and is given in plane-parallel geometry by

$$\eta_E(z) \equiv 2\pi \int_0^\infty dE \int_{-1}^{+1} d\mu \mu E n(z) Q(E) \frac{\partial}{\partial \tau} \Phi(\tau, E, \mu) . \quad (43)$$

The ionization rate, η_i , is defined as the number of electron-ion pairs produced per unit volume per unit time. This can be found to a good approximation from η_E by using Bethe's formula²¹

$$\eta_i(z) = \eta_E(z)/E_s , \quad (44)$$

where E_s is a constant. A good value for E_s for auroral electrons has been found to be 34 eV. In this way we find an approximate formula for η_i without solving explicitly for the secondary electron flux.

8. SOLUTIONS FOR SPECIFIC INCIDENT ELECTRON FLUXES

8.1 Preliminary Remarks

In this section we give analytic expressions for the quantities defined in Section 7 for several specific forms of the incident electron flux. Before we do so, we remind the reader that our analytic solution for the electron flux is only valid for $E > E_{\min}$. However, in the energy integral from 0 to ∞ which defines η_E , we note that the contribution to the integral below E_{\min} only amounts to a few percent for auroral electrons.

21. Bethe, H. A. (1933) Hanbuch der Physik, Verlag Julius Springer, Berlin
24:491.

8.2 Unidirectional-Monoenergetic Incident Flux

For a unidirectional-monoenergetic electron flux incident at the top of the ionosphere the boundary condition is

$$\Phi(E, \mu) = \left(\frac{Q_s}{2\pi E_o \mu_o} \right) \delta(E - E_o) \delta(\mu + \mu_o) , \quad (45)$$

where Q_s is the total energy flux in the downward direction, E_o is the electron energy, and μ_o is the cosine of the angle of incidence, χ , where $0 \leq \chi < \pi/2$. The electron flux is

$$\begin{aligned} \Phi(\tau, E, \mu) = & \left(\frac{Q_s}{2\pi E_o \mu_o} \right) \delta(\mu + \mu_o) \left\{ \delta(E - E_o) \exp(\tau/\mu) \right. \\ & \left. + \sum_{n=1} \delta(E + nW - E_o) b_{n1}(E) [H_n(\tau/\mu, E) - H_n(0, E) \exp(\tau/\mu)] \right\} . \end{aligned} \quad (46)$$

The hemispherical flux is

$$\begin{aligned} \Phi_H(\tau, E) = & \left(\frac{Q_s}{2\pi E_o \mu_o} \right) \left\{ \delta(E - E_o) \exp(-\tau/\mu_o) \right. \\ & \left. + \sum_{n=1} \delta(E - (E_o - nW)) b_{n1} [H_n(-\tau/\mu_o, E) - H_n(0, E) \exp(-\tau/\mu_o)] \right\} . \end{aligned}$$

The energy deposition rate is

$$\begin{aligned} n_E(z) = & \left(\frac{Q_s}{\mu_o} \right) Q(E_o) n(z) \left\{ \exp(-\tau(z, E_o)/\mu_o) + \sum_{n=1} (1 - nW/E_o) b_{n1}^2(E_o - nW) \right. \\ & \times [I_n(-\tau(z, E_o - nW)/\mu_o, E_o - nW) - H_n(0, E_o - nW) \\ & \left. \times \exp(-\tau(z, E_o - nW)/\mu_o)] \right\} , \end{aligned} \quad (48)$$

where the I functions are

$$I_n(x, E) \equiv \frac{\partial}{\partial x} H_n(x, E) . \quad (49)$$

It should be pointed out here that the above sums do not extend to ∞ but to a maximum value, N , given by $NW = E_o - E_{\min}$.

8.3 Isotropic-Maxwellian Incident Flux

For an isotropic-Maxwellian electron flux incident at the top of the ionosphere the boundary condition is

$$\Phi(E, \mu) = \left(\frac{Q_s}{2\pi E_o^3} \right) E \exp(-E/E_o) , \quad \text{for } -1 \leq \mu < 0 , \quad (50)$$

where Q_s is the total energy flux in the downward direction and E_o is the characteristic energy. The resulting electron flux is given by

$$\begin{aligned} \Phi(\tau, E, \mu) = & \left(\frac{Q_s}{2\pi E_o^3} \right) \left\{ E \exp(-E/E_o) \exp(\tau/\mu) + \sum_{n=1}^{\infty} (E + nW) \right. \\ & \times \exp(-(E + nW)/E_o) b_{n1} [H_n(\tau/\mu, E) - H_n(0, E) \exp(\tau/\mu)] \Big\} , \end{aligned} \quad (51)$$

with $\Phi = 0$ for $0 \leq \mu \leq 1$. The hemispherical flux is

$$\begin{aligned} \Phi_H(z, E) = & \left(\frac{Q_s}{2\pi E_o^3} \right) \left\{ E \exp(-E/E_o) E_2(\tau) + \sum_{n=1}^{\infty} (E + nW) \right. \\ & \times \exp(-(E + nW)/E_o) b_{n1} [K_n(\tau, E) - H_n(0, E) E_2(\tau)] \Big\} , \end{aligned} \quad (52)$$

where $E_2(x)$ is the second exponential integral function defined by

$$E_2(x) = \int_1^{\infty} dt t^{-2} \exp(-xt) . \quad (53)$$

The first three K-functions are

$$K_1(x, E) = a_{11}E_2(b_{11}x) \quad , \quad (54)$$

$$K_2(x, E) = a_{22}a_{21}E_2(b_{21}x) - a_{22}a_{11}E_2(b_{11}x) \quad , \quad (55)$$

$$\begin{aligned} K_3(x, E) &= a_{33}a_{32}a_{31}E_2(b_{31}x) - a_{33}a_{32}a_{11}E_2(b_{11}x) \\ &\quad - a_{33}a_{22}a_{21}E_2(b_{21}x) + a_{33}a_{22}a_{11}E_2(b_{11}x) \quad , \end{aligned} \quad (56)$$

The general rule for the K functions is the same as that for the H functions with the exponential function replaced by the second exponential integral function.

The energy deposition rate is

$$\begin{aligned} \eta_E(z) &= \left(\frac{Q_s}{\pi E_o^3} \right) n(z) \int_{E_{\min}}^{\infty} dE E Q(E) \left\{ E \exp(-E/E_o) E_2(\tau) \right. \\ &\quad \left. + \sum_{n=1}^{\infty} (E + nW) \exp(-(E + nW)/E_o) b_{n1} [L_n(\tau, E) - H_n(0, E) E_2(\tau)] \right\} . \end{aligned} \quad (57)$$

The rule for the L functions is the same as that for the I functions except that the exponential function is replaced by the second exponential integral function. In performing the integral over the total inelastic cross section, Q, the integral may be truncated at some E_{\max} . When this is done the infinite sum terminates at a maximum value, N, given by $NW = E_{\max} - E_{\min}$.

8.4 Isotropic-Monoenergetic Incident Flux

For an incident isotropic-monoenergetic flux the boundary condition is

$$\Phi(E, \mu) = \left(\frac{Q_s}{\pi E_o} \right) \delta(E - E_o) \quad \text{for} \quad -1 \leq \mu < 0 \quad , \quad (58)$$

where Q_s is the total energy flux in the downward direction and E_o is the electron energy. The expression for Φ is

$$\Phi(\tau, E, \mu) = \left(\frac{Q_S}{\pi E_0} \right) \left\{ \delta(E - E_0) \exp(\tau/\mu) + \sum_{n=1}^{\infty} \delta(E + nW - E_0) b_{n1} \right. \\ \times [H_n(\tau/\mu, E) - H_n(0, E) \exp(\tau/\mu)] \left. \right\} , \quad (59)$$

with $\Phi = 0$ for $0 \leq \mu \leq 1$.

9. RELATIONSHIP BETWEEN THE ENERGY DEPOSITION RATE AND CHAPMAN AND J FUNCTIONS

9.1 Preliminary Remarks

Chapman functions are functions of altitude which arise in the Chapman theory of the daytime ionosphere. The functions give the ionization rate, which is related to the energy deposition rate, for a single Chapman layer. The ionization rate profile is produced by the photoionization of the neutral particle gas by ionizing electromagnetic radiation from the sun. In the auroral zone at night, the ionized layer is produced by a different process; the precipitation of energetic electrons incident at the top of the atmosphere. It has been known for some time that the auroral ionization rate profile (or energy deposition rate profile) is much more highly peaked as a function of altitude than is a single Chapman function.

In this section we establish the connection between the Chapman functions and the auroral ionization rate, specifically we show that the solution for the energy deposition rate in the auroral ionosphere is a superposition of Chapman functions for unidirectional incident electron fluxes, and a superposition of what we call J functions for isotropic incident electron fluxes. In order to do this we use the alternative expression for η_E we obtain when Eq. (34) is substituted into Eq. (43).

$$\eta_E(z) = 2\pi n(z) \int_{E_{\min}}^{\infty} dE \int_{-1}^0 d\mu E Q(E) \left\{ \Phi(E, \mu) \exp(\tau(z, E) - \mu) \right. \\ + \sum_{n=1}^{\infty} \Phi(E + nW, \mu) \sum_{\ell=1}^n A_{n\ell}(E) \\ \times [B_\ell(E) \exp(B_\ell(E) \tau(z, E)/\mu) - \exp(\tau(z, E) - \mu)] \left. \right\} . \quad (60)$$

9.2 Generalized Chapman and J Functions

The Chapman functions as introduced by Chapman is²²

$$Ch(z) = n(z) \exp \left[-\frac{f}{\mu_0} \int_z^{\infty} dy n(y) \right] , \quad (61)$$

where f is a constant and μ_0 is the cosine of the angle of incidence, χ , where $0 \leq \chi < \pi/2$. Let us now define a generalized Chapman function of three arguments

$$Ch \left(z, \frac{1}{\mu}, f(E) \right) \equiv n(z) \exp \left[\frac{f(E)}{\mu} \int_z^{\infty} dy n(y) \right] , \quad (62)$$

where $0 \leq z < \infty$, $-1 \leq \mu < 0$, and f is a positive function of E , where $0 \leq E < \infty$.

By analogy with the Chapman function let us introduce a J function

$$J(z) \equiv \int_{-1}^0 d\mu n(z) \exp \left[\frac{f}{\mu} \int_z^{\infty} dy n(y) \right] , \quad (63)$$

and a generalized J function

$$J(z, f(E)) \equiv \int_{-1}^0 d\mu n(z) \exp \left[\frac{f(E)}{\mu} \int_z^{\infty} dy n(y) \right] , \quad (64)$$

where $0 \leq z < \infty$, and f is a positive function of E , where $0 \leq E < \infty$. Transforming Eq. (64) to an integral on t , where $t = -\mu^{-1}$, we see that

$$J(z, f(E)) = n(z) E_2 \left[f(E) \int_z^{\infty} dy n(y) \right] , \quad (65)$$

where E_2 is defined by Eq. (53).

22. Chapman, S. (1931) The absorption and dissociative or ionizing effect of monochromatic radiation in an atmosphere on a rotating Earth, Proc. Phys. Soc. 43:26.

9.3 Energy Deposition Rate for Unidirectional Incident Fluxes

For a unidirectional incident flux ($\mu_o = \cos \chi$, $0 \leq \chi < \pi/2$) the energy deposition rate given by Eq. (60) is

$$\begin{aligned} \eta_E(z) = & 2\pi \int_{E_{\min}}^{E_{\max}} dE E Q(E) \left\{ \Phi(E) \operatorname{Ch} \left(z, -\frac{1}{\mu_o}, Q(E) \right) \right. \\ & + \sum_{n=1}^N \sum_{\ell=1}^n \Phi(E + nW) A_{n\ell}(E) \\ & \times \left. \left[B_\ell(E) \operatorname{Ch} \left(z, -\frac{1}{\mu_o}, B_\ell(E) Q(E) \right) - \operatorname{Ch} \left(z, -\frac{1}{\mu_o}, Q(E) \right) \right] \right\}. \end{aligned} \quad (65)$$

Thus, the exact solution of Eq. (16) yields the energy deposition rate as an energy integral over a finite superposition of generalized Chapman functions.

The explicit solution for a unidirectional-monoenergetic incident flux is

$$\begin{aligned} \eta_E(z) = & \left(\frac{Q_s}{\mu_o} \right) Q(E_o) \left\{ \operatorname{Ch} \left(z, -\frac{1}{\mu_o}, Q(E_o) \right) \right. \\ & + \sum_{n=1}^N \sum_{\ell=1}^n (1 - nW/E_o) B_\ell(E_o - nW) A_{n\ell}(E_o - nW) \\ & \times \left. \left[B_\ell(E_o - nW) \operatorname{Ch} \left(z, -\frac{1}{\mu_o}, B_\ell(E_o - nW) Q(E_o - nW) \right) \right. \right. \\ & \left. \left. - \operatorname{Ch} \left(z, -\frac{1}{\mu_o}, Q(E_o - nW) \right) \right] \right\}. \end{aligned} \quad (67)$$

This explicit solution reduces to a finite superposition of generalized Chapman functions with shifted energy arguments.

9.4 Energy Deposition Rate for Isotropic Incident Fluxes

For an isotropic incident flux the energy deposition rate is

$$n_E(z) = 2\pi \int_{E_{\min}}^{E_{\max}} dE E Q(E) \left\{ \Phi(E) J(z, Q(E)) + \sum_{n=1}^N \sum_{\ell=1}^n \Phi(E + nW) A_{n\ell}(E) \times [B_\ell(E) J(z, B_\ell(E) Q(E)) - J(z, Q(E))] \right\} . \quad (68)$$

Here, the exact solution of Eq. (16) yields an energy deposition rate as an energy integral over a finite sum of generalized J functions.

For an isotropic-Monoenergetic incident flux the energy integral can be done explicitly and for an isotropic-Maxwellian incident flux the energy integral can be done by quadrature.

10. USE OF PSEUDOPARTICLES TO APPROXIMATE THE SUMS

In the formulae of Sections 6 through 9, W is a number on the order of 40 eV and the primary auroral electron energies range from about 1 to 60 KeV. As a result, the sums in the formulas extend to as many as 1500 terms representing as many as 1500 scatterings before an energetic electron loses all its energy. However, it turns out that a good approximation to these large sums may be obtained by introducing the notion of pseudoparticles which, in turn, allows us to take many fewer terms in each sum. A pseudoparticle is a particle which has a cross section W/W_p times smaller than the real particle but has an average energy loss per inelastic collision W_p/W times greater, such that the product of the two remains the same. With this approximation a good answer is obtained for the sums given in Sections 6 through 9 with many fewer terms in each sum.

In order to introduce pseudoparticles into the equations of Sections 6 through 9 we simply replace Q by Q_p and W by W_p , that is,

$$Q(E) \rightarrow Q_p(E) \equiv (W/W_p) Q(E) , \quad (69)$$

$$W \rightarrow W_p \equiv (W_p/W) W . \quad (70)$$

We have examined the convergence of the pseudoparticle method as we approximate the sums by a smaller and smaller number, N , of pseudoscatteings

spanning the energy range from E_{\max} to E_{\min} . We have found that a good answer can be obtained with a surprisingly small number of pseudoscatterings. For example, for an isotropic-Maxwellian incident flux with E_0 ranging between 1 and 10 KeV only 10 to 15 pseudoscatterings spanning the energy range are needed to obtain answers to within a few percent of the full solution at most altitudes of interest.

In Figure 1 we show the hemispherically averaged partial fluxes, ϕ_{Hn} , for a sequence of n values for an isotropic-Maxwellian incident flux with $E_0 = 2$ KeV and $Q_s = 1 \text{ erg/cm}^2\text{s}$ for the case where $N = 12$. That is to say, 12 pseudoscatterings spanning the energy range of interest from $E_{\max} = 13$ KeV to $E_{\min} = 1$ KeV. In Figure 2 we illustrate the rate of convergence of Φ_H by showing the sequence of partial sums of ϕ_{Hn} for the same case. In Figure 3 we show the partial ionization rates ($\eta_{in} = \eta_{Eh}/34$) for the same case. Note that for η_{io} we obtain a J function profile and for η_{in} ($n \geq 1$) we obtain functions with a single node, each of which subtracts from η_{io} at high altitudes and adds to η_{io} at low altitudes. In Figure 4 we show the rate of convergence of η_i by showing the sequence of partial sums of η_{in} for the above case.

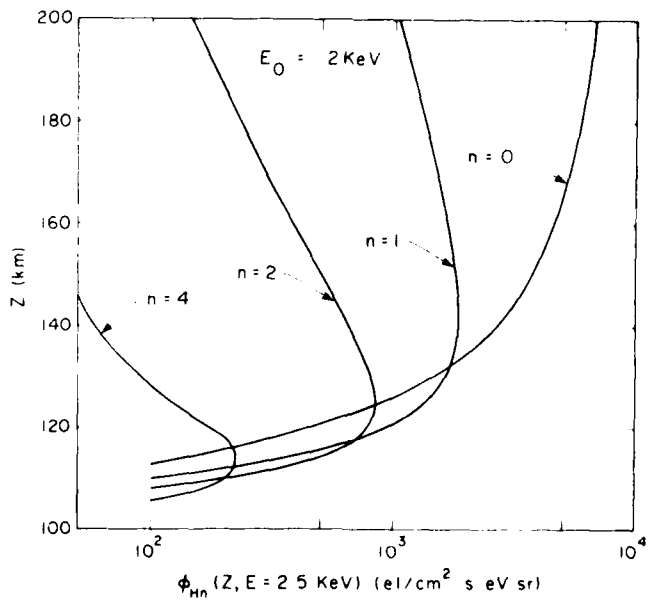


Figure 1. Hemispherically Averaged Partial Fluxes for an Isotropic Maxwellian with $E_0 = 2$ KeV, $Q_s = 1 \text{ erg/cm}^2\text{s}$ and $N = 12$

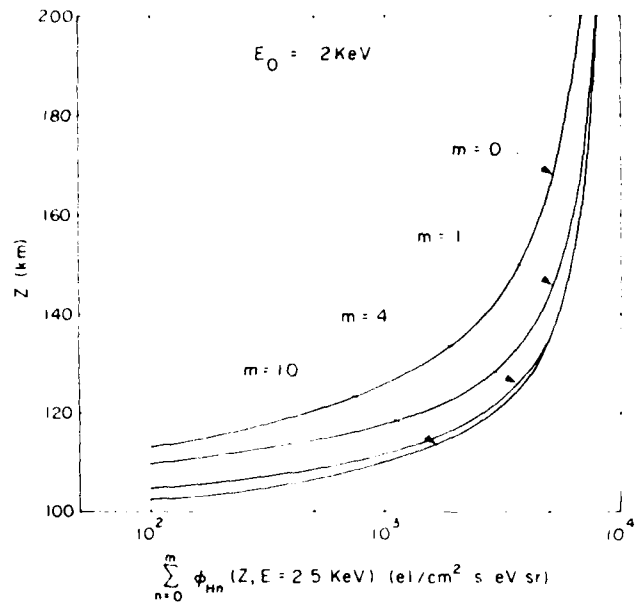


Figure 2. Sequence of Partial Sums of Hemispherically Averaged Partial Fluxes for an Isotropic-Maxwellian as in Figure 1

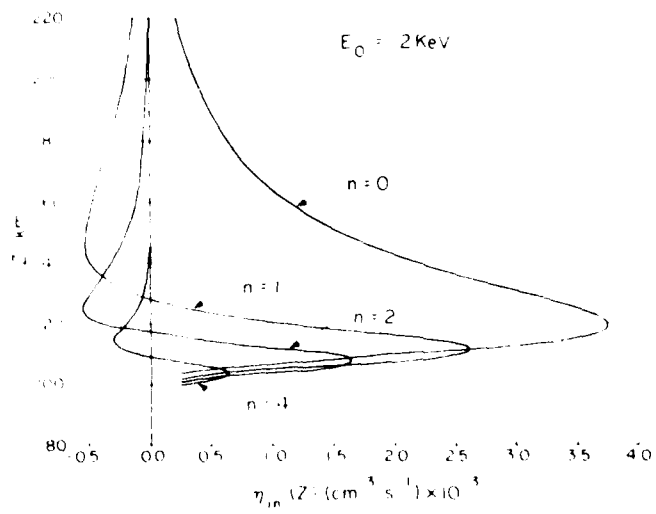


Figure 3. Partial Ionization Rates for an Isotropic-Maxwellian with $E_0 = 2 \text{ KeV}$, $Q_s = 1 \text{ erg/cm}^2 \text{ s}$ and $N = 12$

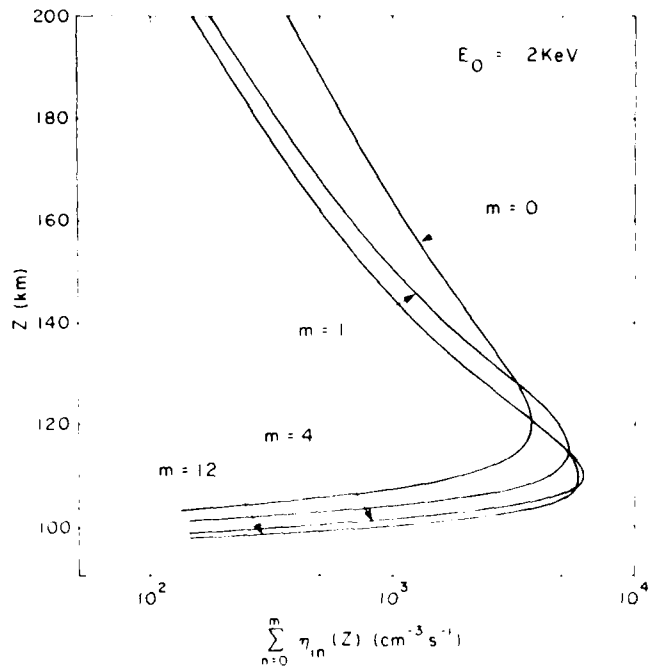


Figure 4. Sequence of Partial Sums of Partial Ionization Rates for an Isotropic-Maxwellian as in Figure 3

As a general rule we find that the lower the altitude the more pseudoscatterings (the larger the N) covering the range from E_{\max} to E_{\min} are needed to obtain a good answer. For example, we find that in the above case the difference in the energy deposition rate for $N = 12$ and $N = 20$ is -0.25 percent at 160 km, +0.8 percent at 110 km and +1.6 percent at 104 km.

II. COMPARISONS

II.1 Preliminary Remarks

In this section, we compare our analytical results to other transport calculations. Quantities of interest are the electron flux, its hemispherically averaged value, and the energy deposition rate. Selected comparisons will be made for monoenergetic and Maxwellian sources.

The particular models we use for comparisons are the Rees, Range, and Strickland models. A Range model was specifically developed for this work and to follow will be a brief description of its contents. We start with the loss

function, $L(E)$, which one can obtain from the Bethe formula²¹ for energies above several hundred eV or from cross sections using

$$L(E) = \sum_k W_k Q_{exk}(E) + \sum_\ell \int dE' (E - E') \sigma_{\ell\ell}^{(p)}(E, E') . \quad (71)$$

$L(E)$ has been calculated from the cross sections in Strickland et al, for N_2 , and from current tabulations for O_2 and O .¹² The formula needed to specify the energy loss is

$$E(z, E_o, \mu_o) = E_o - \sum_j \int_z^{z_o} dz' \mu_o^{-1} L_j(E(z', E_o, \mu_o)) n_j(z') , \quad (72)$$

where μ_o is the cosine of incident angle, z is altitude, E_o is the starting energy at z_o , and $n_j(z)$ is the particle density of the j th neutral species. The energy deposition rate is

$$\eta_E(z) = \int dE_o \int d\Omega_o \sum_j n_j(z) \Phi(E_o, \mu_o) L_j(E(z, E_o, \mu_o)) . \quad (73)$$

For all four models compared in this section the Jacchia (1000°)²³ model atmosphere was used. For the Strickland and Range models the same individual inelastic cross sections and constituent neutral densities were used and for the analytic model the same total inelastic cross section was used. The weighted total inelastic cross section, $Q(E)$, was 2.83, 1.31, 0.568, 0.221, 0.0895, and 0.0297 times 10^{-16} in cm^2 for 0.3, 1, 3, 10, 30, and 100 KeV, respectively. The value used for E_s was 34 eV and the values used for W are given in Section 4.

11.2 Comparisons for Isotropic-Monoenergetic Incident Fluxes

The models to be considered are the analytic, Rees, and Range models. Incident energies to be considered are 2, 5, and 10 KeV. Figure 5 shows η_E vs z for incident power densities of 1 erg/cm²s. The Rees results were generated by us using his energy dissipation function. The analytic and Range results are similar as expected since the corresponding models both contain the forward

23. Jacchia, L.G. (1977) Thermospheric temperature, density, and composition: new models, Rep. 375, Smithson. Astrophys. Observ., Cambridge, Mass.

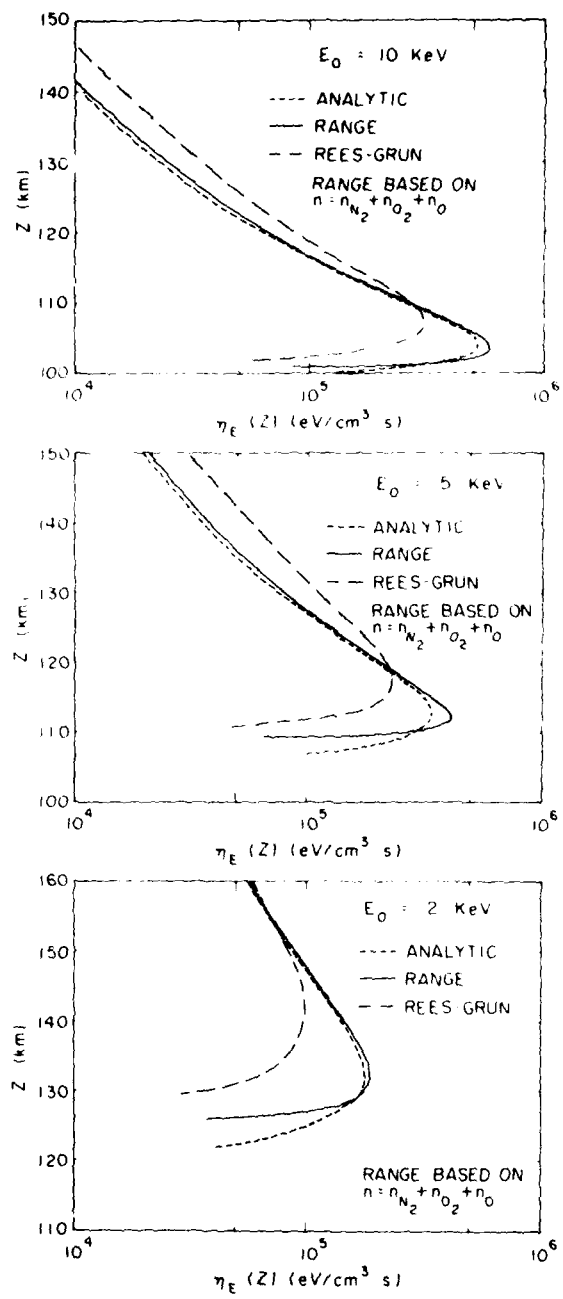


Figure 5. Energy Deposition Rates from the Analytic, Range, and Rees Models for 10, 5, and 2 KeV Isotropic-Monogeneretic Sources Each Containing 1 erg/cm²s

scattering approximation. Departures result from the differences in the description of energy loss. The analytic model allows for discrete energy loss and in turn straggling. Greater differences exist between the analytic and Rees results, the latter showing a broader deposition profile with less total energy deposition. We expect these latter results to be the more accurate since they include the effect of pitch angle scattering.

11.3 Comparisons for Isotropic-Maxwellian Incident Fluxes

The models to be considered are the analytic, Range, and Strickland models. Characteristic energies to be considered are 1, 2, and 5 KeV. Figure 6 shows the incident isotropic-Maxwellian distributions for these energies. Again, the incident power densities are 1 erg/cm²s. Figure 7 shows η_E vs z for the three models and three incident fluxes. These results exhibit basically the same behavior as those appearing in Figure 5. The Strickland results give a broader distribution with a smaller total energy deposition rate due to pitch angle scattering, contained in his model. For all the analytical results of this section, 12 pseudoscatterings were used spanning the range from 1 to 13 KeV. Based upon our studies 12 pseudoscatterings give a solution of Eq. (16) to within about 2 percent for all altitudes above 104 km.

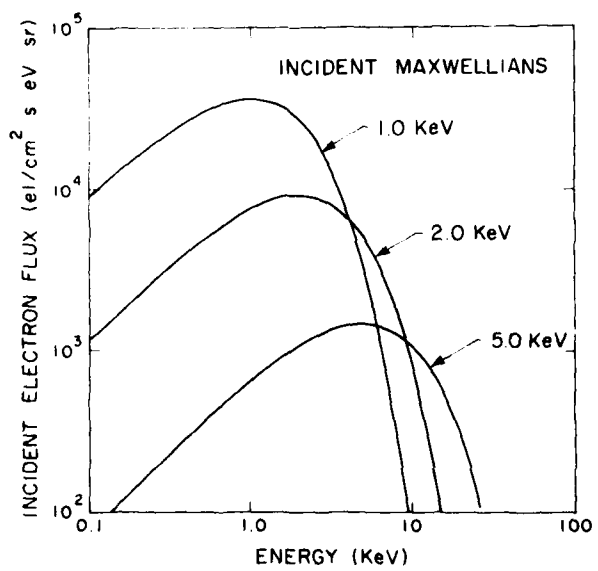


Figure 6. Incident Maxwellian Energy Distributions for Characteristic Energies of 5, 2, and 1 KeV Each Containing 1 erg/cm²s

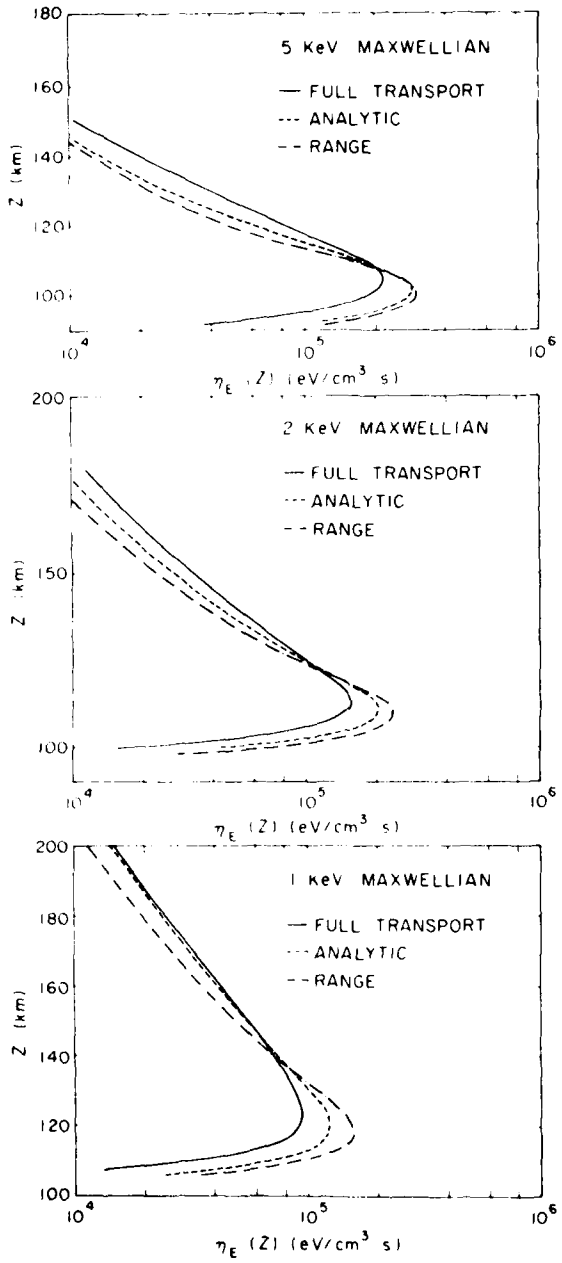


Figure 7. Energy Deposition Rates from the Analytic, Range, and Strickland Models for the 5, 2, and 1 KeV Isotropic-Maxwellian Sources as in Figure 6

We are interested in knowing how well the analytic model does on the electron flux itself. Since the model contains the forward scattering approximation, we are specifically referring to the downward moving flux. To investigate this point, fluxes from the analytic and Strickland models have been compared at selected altitudes and energies. Figure 8 allows for such a comparison at 110 km, for the 2 KeV isotropic-Maxwellian case. As expected, the analytic results are high near $\mu \approx 1$ and low as $\mu \rightarrow 0$ due to the forward-scattering approximation. The differences increase with decreasing energy since scattering becomes more important at low energy. Figure 9 shows the hemispherically averaged flux for the two models from ~ 1 to 10 KeV at 110 and 160 km.

12. CONCLUSION

From the preceding results we conclude that the forward scattering and average discrete energy-loss approximations, which at first seem quite severe, together with the pseudoparticle method of approximating the sums, produce a solution for the primary auroral electron flux in the downward hemisphere which is quite simple to use and is surprisingly close to most of the detailed numerical results of Strickland et al.¹² The formulae we give for the primary auroral electron flux and the quantities derived from it give us insight into the physics of the electron precipitation process and also provide a means of making rapid calculations for the purpose of analyzing auroral data. We also hope that the reader will find the results presented in this paper useful in further auroral studies.

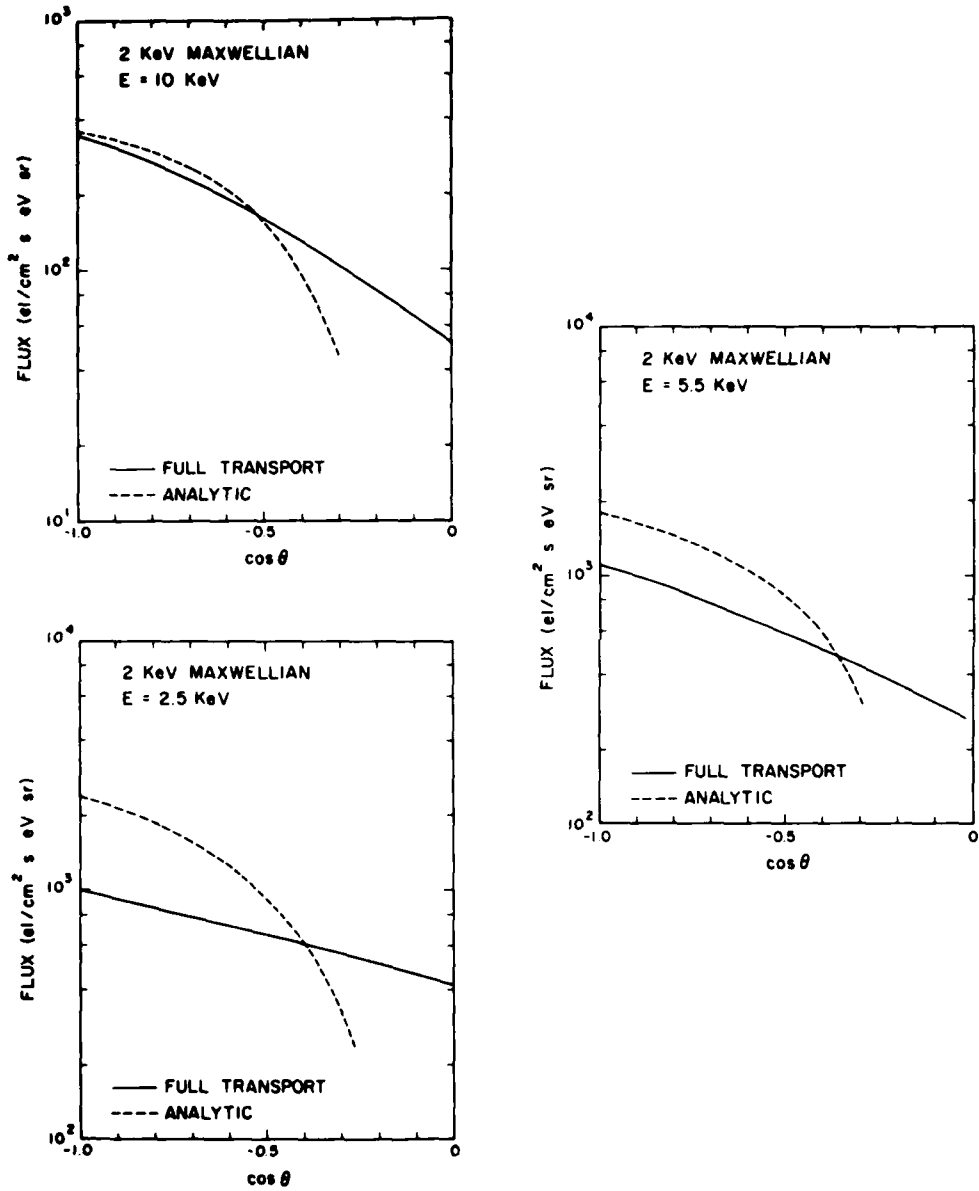


Figure 8. Differential Electron Fluxes from the Analytic ($N = 12$) and Strickland Models at 110 km for the 2 KeV Isotropic-Maxwellian Source

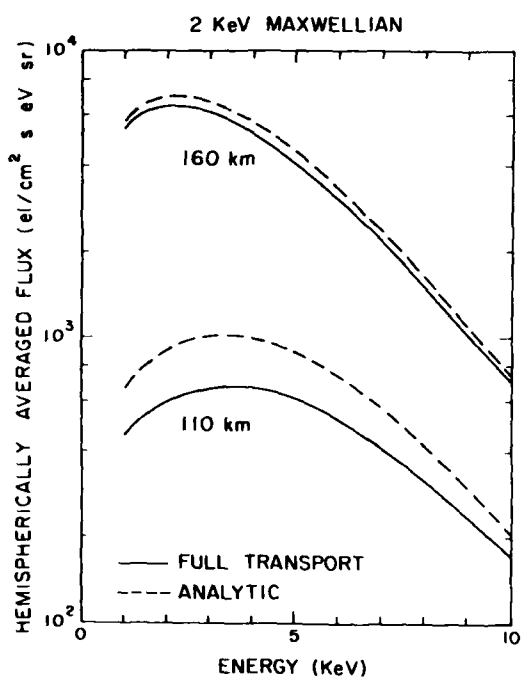


Figure 9. Hemispherically Averaged Fluxes from the Analytic ($N = 12$) and Strickland Models at 110 and 160 km for the 2 KeV Isotropic-Maxwellian Source

References

1. Chamberlain, J.W. (1961) Physics of Aurora and Airglow, Academic Press, N.Y.
2. Spencer, L.V. (1955) Theory of electron penetration, Phys. Rev. 98:1597.
3. Spencer, L.V. (1959) Energy dissipation by fast electrons, National Bureau of Standards Monograph 1.
4. Rees, M.H. (1963) Auroral ionization and excitation by incident energetic electrons, Planet. Space Sci. 11:1209.
5. Grun, A.E. (1957) Lumineszenz-photometrische messungen der energieabsorption im strahlungsfeld von electronquellen, eindimensionaler fall in luft, Z. Naturforsch., Ser. A, 12:89.
6. Walt, M., MacDonald, W.M., and Francis, W.E. (1967) Penetration of auroral electrons into the atmosphere, Physics of the Magnetosphere, R.L. Carovillano, J.F. McClay, and H.R. Radoski, eds., D. Reidel, Dordrecht, Netherlands, 534.
7. MacDonald, W.M. and Walt, M. (1961) Distribution function of magnetically confined electrons in a scattering atmosphere, Ann. Phys. 15:44.
8. Banks, P.M., Chappell, C.R., and Nagy, A.F. (1974) A new model for the interaction of auroral electrons with the atmosphere: Spectral degradation backscatter, optical emission, and ionization, J. Geophys. Res. 79:1459.
9. Banks, P.M. and Nagy, A.F. (1970) Concerning the influence of elastic scattering upon photoelectron transport and escape, J. Geophys. Res. 75:1902.
10. Berger, M.J., Seltzer, S.M., and Maeda, K. (1970) Energy deposition by auroral electrons in the atmosphere, J. Atmos. Terr. Phys. 32:1015.
11. Berger, M.J., Seltzer, S.M., and Maeda, K. (1974) Some new results on electron transport in the atmosphere, J. Atmos. Terr. Phys. 36:591.
12. Strickland, D.J., Book, D.L., Coffey, T.P., and Fedder, J.A. (1976) Transport equation techniques for the deposition of auroral electrons, J. Geophys. Res. 81:2755.

13. Mantas, G.P. (1975) Theory of photoelectron thermalization and transport in the ionosphere, Planet. Space Sci. 23:337.
14. Stammes, K. (1978) A theoretical investigation of the interaction of auroral electrons with the atmosphere, Ph.D. thesis, University of Colorado, Colorado.
15. Davison, B. (1957) Neutron Transport Theory, Oxford Press, London.
16. Opal, C.B., Peterson, W.K., and Beatty, E.C. (1971) Measurements of secondary-electron spectra produced by electron impact ionization of a number of simple gases, J. Chem. Phys. 55:4100.
17. Goudsmit, S. and Saunderson, J.L. (1940) Multiple scattering of electrons, Phys. Rev. 57:24.
18. Wang, M.C. and Guth, E. (1951) On the theory of multiple scattering, particularly of charged particles, Phys. Rev. 84:1092.
19. Fano, U. (1953) Degradation and range straggling of high-energy radiations, Phys. Rev. 92:330.
20. Case, K.M. and Zweifel, P.L. (1967) Linear Transport Theory, Addison-Wesley, Reading, 48.
21. Bethe, H.A. (1933) Handbuch der Physik, Verlag Julius Springer, Berlin 24:491.
22. Chapman, S. (1931) The absorption and dissociative or ionizing effect of monochromatic radiation in an atmosphere on a rotating Earth, Proc. Phys. Soc. 43:26.
23. Jacchia, L.G. (1977) Thermospheric temperature, density, and composition: new models, Rep. 375, Smithson. Astrophys. Observ., Cambridge, Mass.

